THE EFFECT OF CTAB SURFACTANT ADDITION AND ADDITIONAL Sr ON PHASE FORMATION AND MAGNETIC PROPERTIES OF NANOSIZED $SrFe_{12}O_{19}$ SYNTHESIZED VIA SOL-GEL AUTO-COMBUSTION METHOD

Z. Ghiami[1], S. M. Mirkazemi[2] and S. Alamolhoda [*2]

* *alamolhoda@iust.ac.ir*

Received: January 2015 **Accepted: March 2015**

[1] Department of Materials Engineering, Najafabad Branch, Islamic Azad University, Isfahan, Iran.

[2] School of Metallurgy and Materials Engineering, Iran University of Science & Technology (IUST), Tehran, Iran.

Abstract: *Strontium hexaferrite ($SrFe_{12}O_{19}$) nanosized powders were synthesized by sol-gel auto-combustion method with and without cetyltrimethylammonium boromide (CTAB) addition in the sol with Fe/Sr ratio of 11 (using additional Sr). The resultant powders were investigated by X-ray Diffraction (XRD), Transmission Electron Microscope (TEM), Field Emission Scanning Electron Microscope (FESEM) and Vibration Sample Magnetometer (VSM) techniques. Phase constituents of the synthesized samples which were heat treated at temperatures in the range of 700- 900 ◦C were studied. XRD results revealed that CTAB addition facilitates the formation of single phase strontium hexaferrite at 800 ◦C. Microstructural evaluations with FESEM represented that CTAB addition causes formation of larger particles with a narrower size distribution. VSM results represented that the highest amount of intrinsic coercivity force ($_iH_C$) was obtained in the sample without CTAB addition and with additional Sr, calcined at 800 ◦C for 1 h which was equal to 5749.21 Oe, while the value of $_iH_C$ was equal to 4950.89 Oe without additional Sr. The amount of maximum magnetization (M_{max}) was raised from 48.41 emu/g to 62.60 emu/g using CTAB and additional Sr. The microstructure and magnetic properties of the samples have been explained.*

Keywords: *Strontium hexaferrite, sol-gel auto-combustion, surfactant, magnetic properties*

1. INTRODUCTION

M- type hexaferrites such as $SrFe_{12}O_{19}$ (SrM ferrite) have attractive magnetic properties such as high intrinsic coercivity force ($_iH_C$) originated from its high magneto-crystalline anisotropy [1]. This ferrite has wide applications as permanent magnet and magnetic recording media. It can also be used as components in microwaves and magneto-optical devices [1-3]. The wide application of this material is due to a combination of high magnetic properties, low cost and high chemical stability [3, 4]. The conventional method of the production of SrM ferrite has disadvantages such as high calcination temperature, large particle size and uncontrolled particle morphology [5, 6]. Since the properties of this material are related to its chemical composition and also size and morphology of the particles, preparation of SrM ferrite powders having high purity, ultrafine size and good magnetic properties have been the focus of recent researches [2, 7]. Numerous preparation methods such as: chemical co-precipitation [8], hydrothermal [9], self-propagating high temperature [10], mechanical alloying [11], and sol-gel auto-combustion [12] have been developed to synthesize this material.

The results revealed that using stoichiometric ratios of Fe and Sr in all wet chemistry base processing routes causes formation of some amount of residual α-Fe_2O_3 as an impurity phase which deteriorates the magnetic properties [1]. The studies of the author revealed that the Fe/Sr ratio of 10 was needed to synthesize SrM ferrite without residual α-Fe_2O_3 phase in the sol-gel auto-combustion process [12].

There are some reports about the effect of surfactant addition on phase evolutions of the samples with Fe/Sr ratio of 10 representing that presence of surfactant reduces the temperature of single phase SrM ferrite formation but the authors did not represent the effect of surfactant on magnetic properties of the synthesized

[DOI: 10.22068/ijmse.12.2.1]

powders [13-15].

Our previous work [16] represented that presence of CTAB in the synthesis process of SrM ferrites with Fe/Sr ratio of 12 (stoichiometric ratio) considerably reduces the amount of residual α-Fe_2O_3 at the calcination temperature of 800 °C and enhances the $_iH_C$ and maximum magnetization (M_{max}). But the results revealed that there is some residual α-Fe_2O_3 even in the samples synthesized at 900 °C. It seems that in order to synthesize single phase strontium hexaferrite, it is needed to reduce the ratio of Fe/Sr from 12. It may be possible to synthesize single phase SrM ferrite with less additional Sr content (using Fe/Sr ratio more than 10) in presence of surfactant addition. Up to the knowledge of the authors the effect of CTAB as a surfactant on phase evolution and magnetic properties of SrM ferrite synthesized with Fe/Sr ratio of 11 had not been studied yet.

In this research nanosized powders of SrM ferrite were synthesized by a sol-gel auto-combustion method. The effect of Fe/Sr mole ratio of 11 in presence of CTAB addition on phase evolution, microstructure and magnetic properties of the nanosized powders of SrM ferrite were studied.

2. EXPERIMENTAL PROCEDURE

2. 1. Sample Synthesis

SrM ferrite nanopowders were synthesized by sol-gel auto-combustion method.

19.16 g $Fe(NO_3)_3.9H_2O$ (99% Merck) and 0.82 g $Sr(NO_3)_2$ (99% Merck) were dissolved into

50 ml distilled water to make an aqueous solution, then citric acid ($C_6H_8O_7$.99% Merck) was added to the above mixture. The molar ratio of Fe/Sr was set to be 11 and 12 in different samples and the nitrate to citrate ratio was fixed to 1:1.

According to the thermochemical concepts from propellant chemistry, the elements H, C, Fe and Ni are considered reducing elements with the corresponding valencies +1, +4, +3 and +2, respectively. The element oxygen is considered as an oxidizing element with the valency −2. The valency of the element nitrogen is considered to be zero [17-19]. Therefore calculations represent that the ratio of fuel to oxidants in this system is equal to 1.23. The pH value of the solution was increased to 7 by addition of ammonia solution. Then $C_{19}H_{42}BrN$ (CTAB) (99% Merck) was added to the solution in some of the samples as surfactant. The resulting sol was heated at 80 °C on magnetic stirrer to form a gel. Then by heating at 300 ºC, the gel undergoes a self-ignition reaction to form a very fine brown foamy powder. Finally, the samples were calcined at temperatures of 700 ºC, 800 ºC and 900 ºC for 1h in air atmosphere.

2. 2. Characterization

The phase identification of the combustion products and calcined powders was performed by X-ray diffraction (XRD) using Philips X'pert Pro X-ray diffractometer using monochromatic Cu-K_α radiation (λ=1.5405Å). Magnetic measurements were taken out at room temperature at the maximum applied field of 14kOe using vibrating sample magnetometer (VSM) model MDK. The morphology of the powders was studied by a transmission electron microscope (TEM) at 200 kV (Philips CM200) and field emission scanning electron microscope (FESEM) model MIRA TESCAN.

3. RESULTS AND DISCUSSIONS

X-ray diffraction patterns of the combustion product and samples calcined at 700 °C, 800 °C and 900 °C for 1 h with molar Fe/Sr ratio of 11 are shown in Fig. 1. The combustion product consists of γ-Fe_2O_3, $SrCO_3$ and α-Fe_2O_3 phases. Presence of γ-Fe_2O_3, α-Fe_2O_3 and $SrFe_{12}O_{19}$ phases could be observed in the samples calcined at 700 °C with and without CTAB addition. Comparing the intensities of the strontium hexafrrite peaks with γ-Fe_2O_3 and α-Fe_2O_3 peaks in both samples calcined at 700°C represents that the intensity of γ-Fe_2O_3 and α-Fe_2O_3 peaks are higher in the sample synthesized without CTAB addition, representing formation of less amount of $SrFe_{12}O_{19}$ in this sample. With increasing the calcination temperature to 800°C there is no sign of α-Fe_2O_3 in the XRD pattern of the sample

[DOI: 10.22068/ijmse.12.2.1]

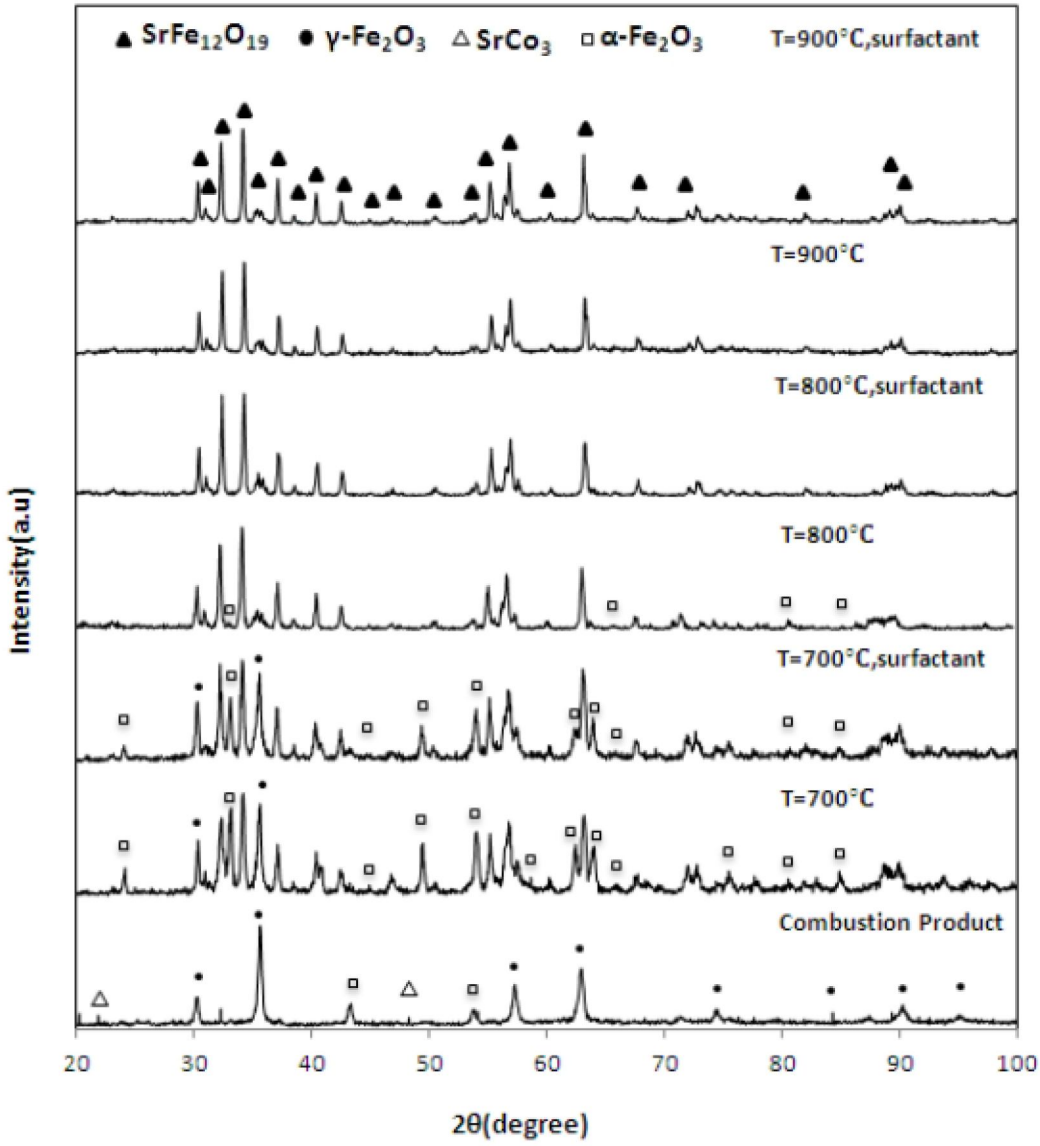

Fig.1. XRD Patterns of the combustion product and the samples synthesized with and without CTAB addition with the Fe/Sr ratio of 11 calcined at 700, 800 and 900 ◦C for 1h.

synthesized with Fe/Sr ratio of 11 with CTAB additions while small signs of presence of α-Fe_2O_3 could be observed in the XRD pattern of the sample synthesized without CTAB addition.

In our previous work [16], XRD patterns represented that there is a small amount of residual

α-Fe_2O_3 in the sample synthesized with CTAB addition with Fe/Sr ratio of 12 calcined at 800°C; while there is a high amount of residual α-Fe_2O_3 in the sample synthesized without CTAB addition at the same conditions. In the sol-gel auto-combustion synthesis some additional Sr is needed to prepare single phase strontium hexaferrite. This is related to the difference in the ability of Sr and Fe ions in the sol to form complexes with citric acid [20] and low solubility of $Sr(OH)_2$ in aqueous solutions [1, 21]. Here the XRD results represent that CTAB additions facilitate the entrance of Sr ions to the reactions

[DOI: 10.22068/ijmse.12.2.1]

of hexaferrite formation by facilitating the solution of Sr ions in the sol. So, both the CTAB addition and decreasing the Fe/Sr ratio to 11 in the sol, facilitate the formation of the single phase hexaferrite at 800°C, while without CTAB addition the single phase SrM ferrite would be formed at the Fe/Sr ratio of 10 [12]. XRD results in Fig. 1 represent that with increasing the calcination temperature to 900 °C there is no sign of presence of α-Fe_2O_3 in both samples.

The FESEM images of the calcined sample are shown in Fig. 2. The porous micro structure of the agglomerates obtained in all the samples may be attributed to the liberation of large quantity of gases produced during the combustion process [22]. The particles appear to be bounded together and formed aggregates. However the observed particles in the sample synthesized with surfactant addition are larger particles with a narrow size distribution while it seems that the size distribution is wide in the sample without CTAB addition. It was reported that addition of cationic surfactant with molecules composed from a hydrophilic head and a hydrophobic tail, into the sol, results in the formation of reverse micelles.

Reverse micelles are nanoscale hydrophilic cavities of microemulsions. These diverse multimolecular structures were used as nano-templates for materials synthesis [23]. Placing the aqueous ions inside these micelles can be effective in controlling the nucleation and growth of particles [14], therefore more uniform particles would be obtained. DTA results of the gels prepared with and without CTAB addition for sol gel auto-combustion synthesis of CuO [22] represented that CTAB addition shifted the exothermic peak of the combustion process to higher temperatures and increased exothermicity of the reaction strongly. This increased liberated heat may leads to formation of larger particles. The above mentioned DTA plots also represented a second exothermic peak of weaker intensity in all of the samples which is related to the burning of the residual organic matter during calcination process. Again the heat release in case of CTAB assisted sample is comparatively higher [22]. Therefore it seems that CTAB addition leads to some remained unreacted organic material that during calcination process decomposes. The thermal energy release due to organic material decomposition, raise the particle crystallinity and causes the reduced formation temperature of strontium hexaferrite. In the synthesis process of strontium hexaferrite via coprecipitation method using CTAB as surfactant, it was observed that CTAB surfactant improves the crystallization of strontium hexaferrite. The samples prepared with

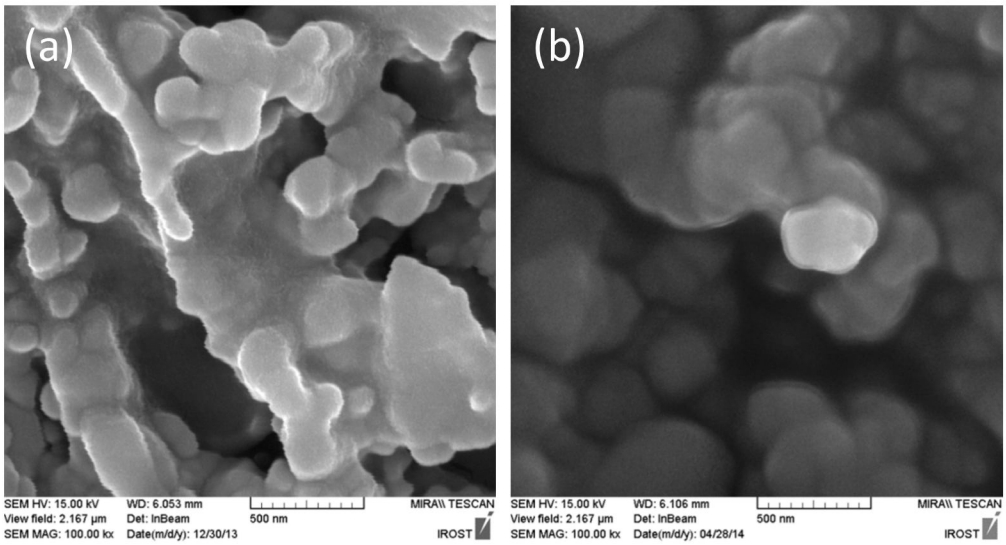

Fig.2. FESEM images of the samples synthesized a) without and b) with CTAB addition calcined at 800 ◦C for 1h.

[DOI: 10.22068/ijmse.12.2.1]

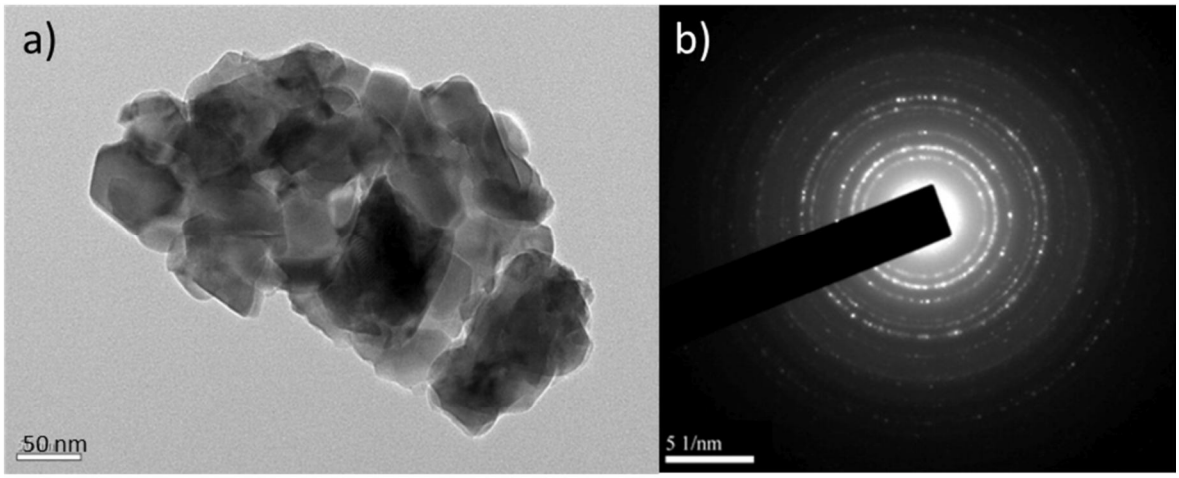

Fig. 3. TEM image of the sample synthesized with CTAB addition calcined at 800◦C for 1h and its related SAED pattern.

CTAB surfactant showed ultrathin hexagonal platelet-like (thickness: 10–20 nm) morphology with particle size of 50–150 nm, whereas other samples synthesized without CTAB addition exhibited rod-like shape with particle size of 40–100 nm [24]. Also more particle growth and higher crystallinity was observed, using excess citric acid in the synthesizing of barium hexaferrite by sol-gel auto-combustion route as a result of increased heat release during combustion and calcination processes [25].

Fig. 3 represents the TEM image of the SrM ferrite powders with CTAB additions, calcined at 800 °C for 1h. The image represents the high aggregation of the particles which is the result of the combustion process. Also the small hexagonal shape particles with nanometric sizes could be observed in this image.

Magnetization curves of the samples are shown in Fig 4. The magnetic properties of the samples with Fe/Sr rato of 11 are listed in table 1. Table 2 represents the $_{i}H_{C}$ and M_{max} values obtained for the sample with Fe/Sr ratio of 12 [16]. The tables represent that with decreasing the ratio of Fe/Sr from 12 to 11, both the $_{i}H_{C}$ and M_{max} values are increased. However there is a bit difference in the values obtained for the samples synthesized with and without CTAB additions with Fe/Sr ratio of 11. The $_{i}H_{C}$ value decreased from 57.5 kOe to 55.9 kOe and the M_{max} value

Table 1. The intrinsic coercivity force (iHc) and maximum magnetization (Mmax) of the samples with Fe/Sr ratio of 11 calcined at 800 and 900°C with (Y) and without (N) CTAB addition

CTAB addition	Calcination Temperature (◦C)	M_{max}(emu/g)	H_c(Oe)
N	800	62.09	5749.21
Y	800	62.60	5593.60
N	900	61.96	5459.02
Y	900	63.34	5177.24

[DOI: 10.22068/ijmse.12.2.1]

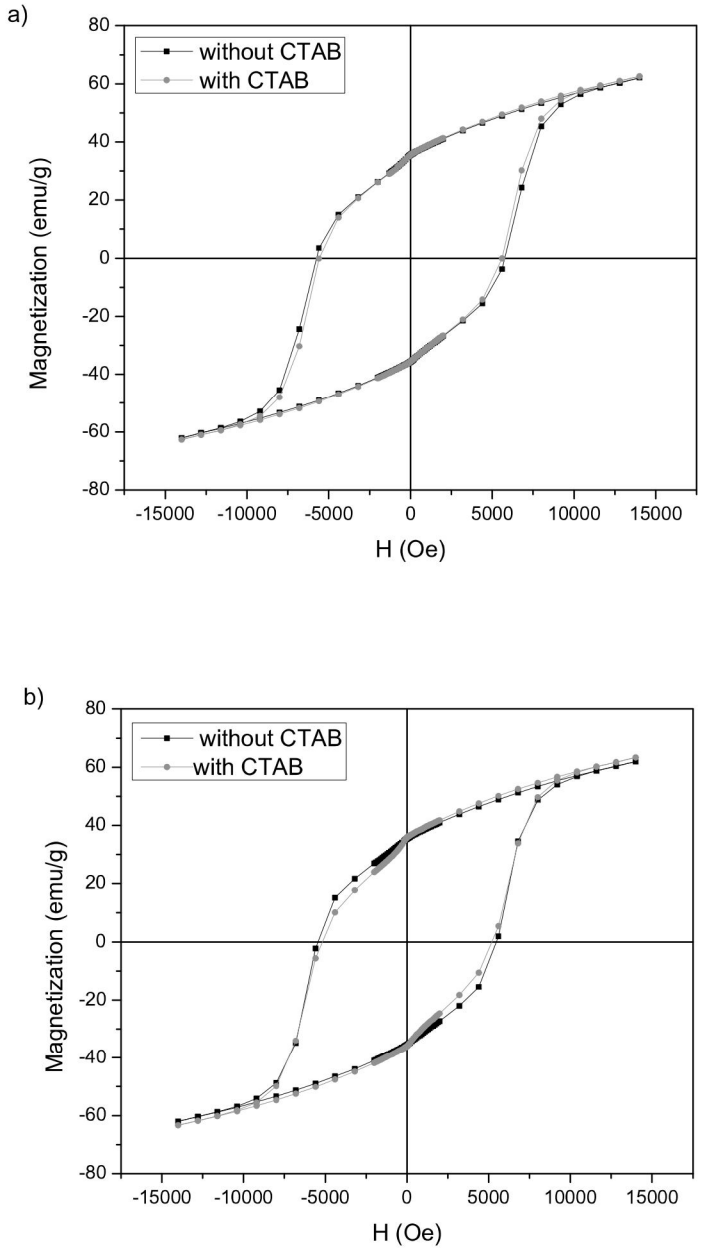

Fig.4. Hysteresis loops of the samples calcined at a) 800 and b) 900 °C with Fe/Sr ratio of 11 without and with CTAB addition.

increased from 62.09 to 62.60emu/g with CTAB addition for the samples synthesized with Fe/Sr ratio of 11. There are several microstructural characteristics that affect the coercivity including crystallinity, morphology, particle size and phase homogeneity [26]. FESEM results represented smaller particles in the sample without CTAB addition so there might be more particles in the single domain size range in this sample which increase the $_iH_C$. Also, there are different reports about the effect of α-Fe_2O_3 phase on the $_iH_C$ of hexaferrites. There is a report representing that $_iH_C$ varies randomly with increasing the content of α-Fe_2O_3 phase coexisting with hexaferrite [27], while there is another report that represents the dilution of hexaferrite with hematite increases

[DOI: 10.22068/ijmse.12.2.1]

Table 2. The intrinsic coercivity force (iHc) and maximum magnetization (Mmax) of the samples with Fe/Sr ratio of 12 calcined at 800 and 900°C with (Y) and without (N) CTAB addition [16]

CTAB addition	Calcination Temperature (◦C)	M_{max}(emu/g)	H_c(Oe)
N	800	48.41	4950.89
Y	800	60.40	5221.47
N	900	61.35	5521.31
Y	900	61.35	4994.77

the $_iH_C$, since the possibility of magnetic flux continuity decreases and isolated grains approach the single domain behavior [28]. Here the variation in $_iH_C$ of the samples is not severe; however the presence of small amount of α-Fe_2O_3 may be effective for approaching the single domain behavior.

The higher crystallinity of the sample synthesized with CTAB additions and also absence of any residual α-Fe_2O_3 phase, a bit enhances the amount of M_{max} [24]. With increasing the calcination temperature to 900 °C the intrinsic coercivity forces of the samples reduced which may be due to grain coarsening and transition of the size of particles from single domain to multi domain. Also the removed residual α-Fe_2O_3 phase may affect the $_iH_C$. The $_iH_C$ of the sample synthesized with CTAB is again lower which may be due to presence of larger particles. However the M_{max} of the sample synthesized with CTAB addition calcined at 900 °C is the highest amount obtained in all samples equal to 63.3 emu/g, which may be due to higher crystallinity of this sample [24]. Also it should be mentioned that there might be some residual α-Fe_2O_3 phase in the sample calcined at 800 °C, which was not in the limitation of XRD detection accuracy which is omitted by calcination at 900 °C. Totally it could be concluded that although CTAB additions have high effect on magnetic properties of the samples synthesized with stoichiometric ratio of Fe/Sr, with decreasing the Fe/Sr ratio to 11 nevertheless the CTAB addition facilitates formation of single phase SrM ferrite at a 800 °C it has not considerable effect on magnetic properties while the change in Fe/Sr ratio from 12 to 11 has more effect on magnetic properties.

CONCLUSION

The $SrFe_{12}O_{19}$ nanosized powders were synthesized by sol-gel auto-combustion method with and without CTAB addition with the Fe/ Sr ratio of 11. The results revealed that both the surfactant addition and increasing the amount of Sr ions in the sol facilitate the formation of the single phase SrM ferrite at 800°C. TEM observations represented formation of nanosized particles of SrM ferrite. Microstructural evaluations with FESEM represented that CTAB addition causes formation of larger particles with a narrower size distribution. VSM results represented that changing the Fe/Sr ratio is more effective on increasing the coersivity force than CTAB addition while both Fe/Sr ratio and CTAB addition are effective factors on increasing of M_{max} quantities since both the factors are effective in removing the residual α-Fe_2O_3. The highest amount of $_iH_C$ is observed in the sample with Fe/Sr ratio of 11 without CTAB addition calcined at 800 °C which is equal to 5593.60 Oe and the highest amount of M_{max} is obtained in the sample with CTAB addition with Fe/Sr ratio of 11 calcined at 900 °C which is equal to 63.34emu/g.

[DOI: 10.22068/ijmse.12.2.1]

REFERENCES

1. Sivakumar, M., Gedanken, A., Zhong, W., Du, Y. W., Bhattacharya, D., Yeshurun, Y. and Felner, I., "Nanophase formation of strontium hexaferrite fine powder by the sonochemical method using Fe(CO)5." J. Magn. Magn. Mater., 2004, 268, 95–104.
2. Wang, Y., Li, Q., Zhang, C. and Li, B., "Effect of Fe/Sr mole ratios on the formation and magnetic properties of $SrFe_{12}O_{19}$ microtubules prepared by sol–gel method". J. Magn. Magn. Mater., 2009, 321, 3368–3372.
3. Ketov, S. V., Yagodkin, Yu. D., Lebed, A. L., Chernopyatova, Yu. V. and Khlopkov, K., "Structure and magnetic properties of nanocrystalline $SrFe_{12}O_{19}$ alloy produced by high-energy ball milling and annealing." J. Magn. Magn. Mater., 2006, 300, e479–e481.
4. Xia, A., Zuo, C., Chen, L., Jin, C. and Lv, Y., "Hexagonal $SrFe_{12}O_{19}$ ferrites: Hydrothermal synthesis and their sintering properties". J. Magn. Magn. Mater., 2013, 332, 186-191.
5. Haberey, F., Kockel, A., "The formation of strontium hexaferrite $SrFe_{12}O_{19}$ from pure iron oxide and strontium carbonate". IEEE Trans. Magn., 1976, 12, 983-985.
6. Zhanyong, W., Liuming Z., Jieli, L., Huichun, Q., Yuli, Z., Yongzheng, F., Minglin, J. and Jiayue, X., "Microwave-assisted synthesis of $SrFe_{12}O_{19}$ hexaferrites". J. Magn. Magn. Mater., 2010, 322, 2782-2785.
7. Sui, X., Scherge, M., Kryder, M. H., Snyder, J. E., Harris, V. G. and Koon N. C., J., "Barium ferrite thin-film recording media". Magn. Magn. Mater. 1996, 155, 132-139.
8. Lu, H. F., Hong, R. Y. and Li, H. Z., "Influence of surfactants on co-precipitation synthesis of strontium ferrite". J. Alloys Compd., 2011, 509, 10127– 10131.
9. Wang, J. F., Ponton, C. B., Grossinger, R. and Harris, I. R., "A study of La-substituted strontium hexaferrite by hydrothermal synthesis". J. Alloys Compd., 2004, 369, 170–177.
10. Elvin, G., Parkin, I. P. P., Bui, Q. T., Barquin, L. F., Pankhurst, Q. A., Komarov, A. V. and Morozov, Y. G., "Self-propagating high-temperature synthesis of $SrFe_{12}O_{19}$ from reactions of strontium superoxide, iron metal and iron oxide powders". J. Mater. Sci. Lett., 1997, 16, 1237-1239.
11. Ding, J., Miao, W.F., McCormick, P.G. and Street, R., "High-coercivity ferrite magnets prepared by mechanical alloying". J. Alloys Compd., 1998, 281, 32-36.
12. Alamolhoda, S., Seyyed Ebrahim,i S. A. and Badiei, A., "Optimization of the Fe/Sr Ratio in Processing of Ultrafine Strontium Hexaferrite Powders by a Sol–Gel Auto combustion Method". Phys. Met. Metall., 2006, 102, S71–S73.
13. Ghobeiti Hasab, M., Seyyed Ebrahimi, S. A. and Badiei, A., "Comparison of the effects of cationic, anionic and nonionic surfactants on the properties of Sr-hexaferrite nanopowder synthesized by a sol–gel auto-combustion method". J. Magn. Magn. Mater., 2007, 316, e13–e15.
14. Ghobeiti Hasab, M., Seyyed Ebrahimi, S. A. and Badiei, A., "The effect of surfactant hydrocarbon tail length on the crystallite size of Sr-hexaferrite powders synthesized by a sol–gel auto-combustion method". J. Magn. Magn. Mater. 2007, 310, 2477–2479.
15. Ghobeiti Hasab, M., Seyyed Ebrahimi, S. A. and Badiei, A., "Effect of different fuels on the strontium hexaferrite nanopowder synthesized by a surfactant-assisted sol–gel auto-combustion method". J. of Non-Cryst. Solids, 2007, 353, 814–816.
16. Mirkazemi, S. M., Alamolhoda, S. and Ghiami, Z., "Microstructure and magnetic properties of $SrFe_{12}O_{19}$ Nano-sized powders prepared by Sol-Gel Auto-combustion method with CTAB surfactant". J Supercond. Nov. Magn,. DOI 10.1007/s10948-014-2872-x.
17. Pillai, V. and Shah, D. O., "Synthesis of high-coercivity cobalt ferrite particles using water-in-oil microemulsions", J. Magn. Magn. Mater., 1996,163, 243-248.
18. Jain, S. R., Adiga, K. C. and PaiVernecker, V. R., "A New Approach to Thermochemical Calculations of Condensed Fuel-Oxidizer Mixtures", Combust. Flame, 1981, 40, 71-79.
19. Jr Franco, A., Alves, T. E. P., Lima, E. C. deO, Nunes, E. daS and Zapf, V., Vivien Zapf, "Enhanced magnetization of nanoparticles of

[DOI: 10.22068/ijmse.12.2.1]

MgxFe(3 −x)O4(0.5 ≤ x ≤ 1.5) synthesized by combustion reaction", Appl. Phys. A, 2009, 94, 131-137.

20. Martell, E. and Smith, R. M., "Critical Stability Constants." Vol. 3, Springer, New York, USA, 1977.
21. Dean, J. A.: Lange's Handbook of Chemistry. 15th edn. Mc Graw Hill, New York, USA, 1999.
22. Singh, I. and Bedi, R. K., "Surfactant-assisted synthesis, characterizations, and room temperature ammonia sensing mechanism of nanocrystalline CuO." Solid State Sci., 2011, 13, 2011-2018.
23. Uskokovic, V., and Drofenik, M., "Synthesis of materials within reverse micells," Surf. Rev. Lett., 2005, 12, 239–277.
24. Chen, D. Y., Meng, Y. Y., Zeng, D. C., Liu, Z. W., Yu, H. Y., Zhong, X. C., "CTAB-assisted low-temperature synthesis of $SrFe_{12}O_{19}$ ultrathin hexagonal platelets and its formation mechanism." Mater. Lett., 2012, 76, 84–86.
25. Mali, A., and Ataie, A., "Influence of the metal nitrates to citric acid molar ratio on the combustion process and phase constitution of barium hexaferrite particles prepared by sol–gel combustion method." Ceram. Int., 2004, 30, 1979–1983.
26. Xu, Y. F., Ma, Y. Q., Xu, S. T., Zan, F. L., Zheng, G. H. and Dai, Z. X., "Effects of vacancy and exchange-coupling between grains on magnetic properties of $SrFe_{12}O_{19}$ and α-Fe_2O_3 composites." Mater Res Bull. 2014, 57, 13-18.
27. Hessien, M. M., Rashad, M. M., El-Barawy, K., "Controlling the composition and magnetic properties of strontium hexaferrite synthesized by co-precipitation method." J. Magn. Magn. Mater., 2008, 320, 336–343.
28. Sánchez-DeJesús F., Bolarín-Miró, A. M., Cortés-Escobedo, C. A., Valenzuela, R., Ammar, S., "Mechanosynthesis, Crystal structure and magnetic characterization of M-type $SrFe_{12}O_{19}$." Ceram. Int., 2014, 40, 4033–4038.

[DOI: 10.22068/ijmse.12.2.1]